RSC Advances

ROYAL SOCIETY OF CHEMISTRY

www.rsc.org/advances

Substituted furopyridinediones as novel inhibitors of α-glucosidase

Chandramohan Bathula,[1, §] Rajanikanth Mamidala,[4, §] Chiranjeevi Thulluri,[3] Rahul Agarwal,[2], Kunal Kumar Jha,[1] Parthapratim Munshi,[1] Uma Adepally,[3] Ashutosh Singh,[2] M. Thirumalachary[4], Subhabrata Sen[1, *]

[1] *Department of Chemistry, School of Natural Sciences, Shiv Nadar University, Chithera, Dadri, UP 201314, India*

[2] *Department of Life Science, School of Natural Sciences, Shiv Nadar University, Chithera, Dadri, UP 201314, India*

[3] *Institute of Science and Technology, Jawaharlal Nehru Technological University Hyderabad, Kukatpally, Hyderabad500085, Telengana, India*

[4] *Department of Chemistry, Jawaharlal Nehru Technological University Hyderabad, Kukatpally, Hyderabad500085, Telengana, India*

[§] Equal Contributor

Abstract

The global preponderance of *diabetes mellitus* has prompted the medical community to opt for various therapeutic solutions to curb the menace. One of the means involved controlling the post prandial hyperglycemia. α-glucosidase inhibitors are known to be excellent agents of controlling postprandial hyperglycemia. Different classes of α-glucosidase inhibitors has been discovered. In this context, a diverse library of substituted furopyridinediones (**12a-v**) was designed as potential inhibitors of α-glucosidase, using an intuitive scaffold hopping approach (which was further rationalized by molecular docking). They were synthesized in one step *via* an aldol condensation reaction of furopyridinedione scaffold and appropriate aldehydes. The compounds were screened against α-glucosidase using acarbose as the reference inhibitor. Among the screened compounds, **12p** transpired to be the lead candidate with an IC_{50} of 0.24 μM. Lineweaver Burke analysis of **12p** indicated it to be a mixed inhibitor. X-ray crystallography of **12p** further confirmed its structure. Molecular modelling studies and molecular dynamic simulation experiments were performed against a homology model of α-glucosidase to observe the binding interaction of **12p** with the enzymes.

Key words

Furopyridinediones, acarbose, mixed inhibitor, α-glucosidase,

Introduction

Type I and type II diabetes or *diabetes mellitus* is one of the most widespread metabolic disorders in the world.[1] Until now, it has affected nearly 200 million global population. It is estimated that this number will swell to ~400 million by 2030.[2] The disease is delineated by hyperglycemia associated with various complications such as cardiac and vascular diseases, thrombosis, cerebral and renal disorders.[3]

The present therapeutic approaches to treat type II diabetes include antidiabetic oral medicines *viz.*α-glucosidase inhibitors, glucosuric thiazolidiene diones and etc.[4] Peptide drugs such as Exenatide (glucagen like peptide-1 (GLP-1_ agonists) and Vildagliptan (dipeptidyl peptidase IV inhibitors) are few of the novel therapies in the market.[5] Finally cannabinoid receptor type I antagonists and bile aid sequestrants are part of emerging therapeutics.[6]

Controlling postprandial hyperglycemia by delaying the digestion of carbohydrates has been an effective therapeutic approaches in type II diabetes.[7] In this respect inhibition of α-glucosidase enzyme slows down the carbohydrate absorption. This stabilizes the blood glucose level among diabetic patients, thereby preventing hyperglycemia.

α-Glucosidase belongs to a class of glycoside hydrolase enzymes that releases glucose by cleaving the glycosidic bond from the nonreducing terminal of their oligomeric substrate.[8] In mammals it degrades glycogen, assists in internal digestion of dietary carbohydrates and in glycoprotein folding and maturation. α-Glucosidase inhibitors (*viz*. acarbose) has been established as an effective medicine in type II diabetes.[9] They inhibit the membrane bound α-glucosidase at the brush border of the small intestine that reduces digestion of starch and other dietary sugars which in turn prevents hyperglycemia and maintains normal blood sugar level.[10]

Apart from established therapies, literature study suggested that diverse heterocycles has been discovered as potent α-glucosidase inhibitors. Ranging from natural imino sugars like 1, 4-dideoxy-1,4-imino-D-arabinitol (DAB) (**1**) (that inhibits yeast α-glucosidase with an IC_{50} of 0.15μM) and 2R, 5R-dihydroxymethyl-3R, 4R-dihydroxypyrrolidine (DMDP) (**2**), (containing an additional hydroxymethyl group and with a potency of 0.7 μM against yeast α-glucosidase) to chalcone glucosides **3a-d** where the inhibitory activity against α-glucosidase reduces with the removal of the galloyl and caffeoyl substituents, flavonoid such as **4 (**Brussochalcone A), a

prenylated compound that inhibits yeast α-glucosidase non-competitively with K_i = 5.3 μM, macrocyclic cyclitol **5** exhibiting potent α-glucosidase activity in rats, (IC_{50} rat intestinal maltase = 0.23 μM), Radicamins A/B, **6a**/**b**, which are alkaloids and isolated from plants also inhibits α-glucosidase in the range of 6.7-9.3 μM, highly active curcumins **7a-c** (inhibits α-glucosidase with an IC_{50} of 1.6→2.3 μM) and synthetic variants like azasugar **8**, oxoindole derivatives **9a-c** (inhibiting yeast α-glucosidase with an IC_{50} of 2-14 μM**)**, terpenes, **10**, and etc (Figure 1).[11-19]

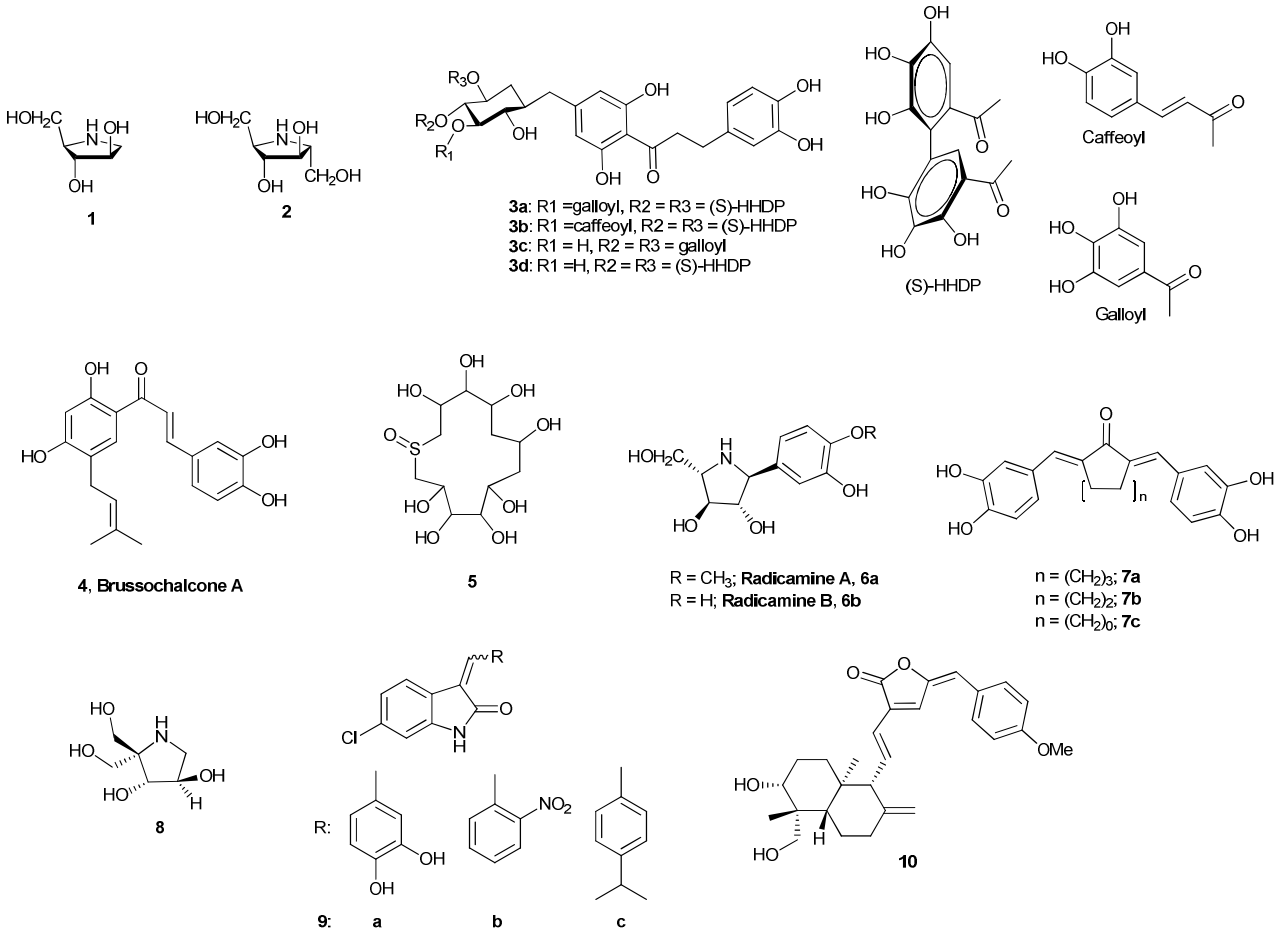

Figure 1. Representative inhibitors of α-glucosidase (natural and synthetic)

In a bid to identify a novel inhibitor of α-glucosidase, a close scrutiny of these natural products and their subsequent comparison with our in-house inventory of scaffolds prompted an intuitive and bioisosteric scaffold hopping exercise based on compounds **7a-c** and **9a**. It resulted in the selection of compound **12d** containing furopyridinedione as the backbone. To rationalize our design, molecular docking revealed strong H-bonding and other nonbonding interactions of the

linker and the backbone of **7a** and **9a** with α-glucosidase (Figure 2 [below] and Table 1 of *SI* 2) (a homology model was developed [refer *SI-2]* where the stereochemical quality of the model was validated by Ramachandran plot and more than 99.3 % residues are in favored and allowed regions and only 0.7% [6 residues]are in outlier region [Figure 1, *SI-2*]. To our extreme gratification compound **12d** also unveiled similar binding interaction with the protein (Figure 2 (below and Table 1 of *SI* 2).

Hence, with **12d** as the reference, a molecular library **12a-v** were envisioned as the potential inhibitors of α-gluosidase. The general design of the compounds comprised of furopyridinedione (**13**) attached to an aromatic or heteroaromatic moiety through a double bond (Figure 2).

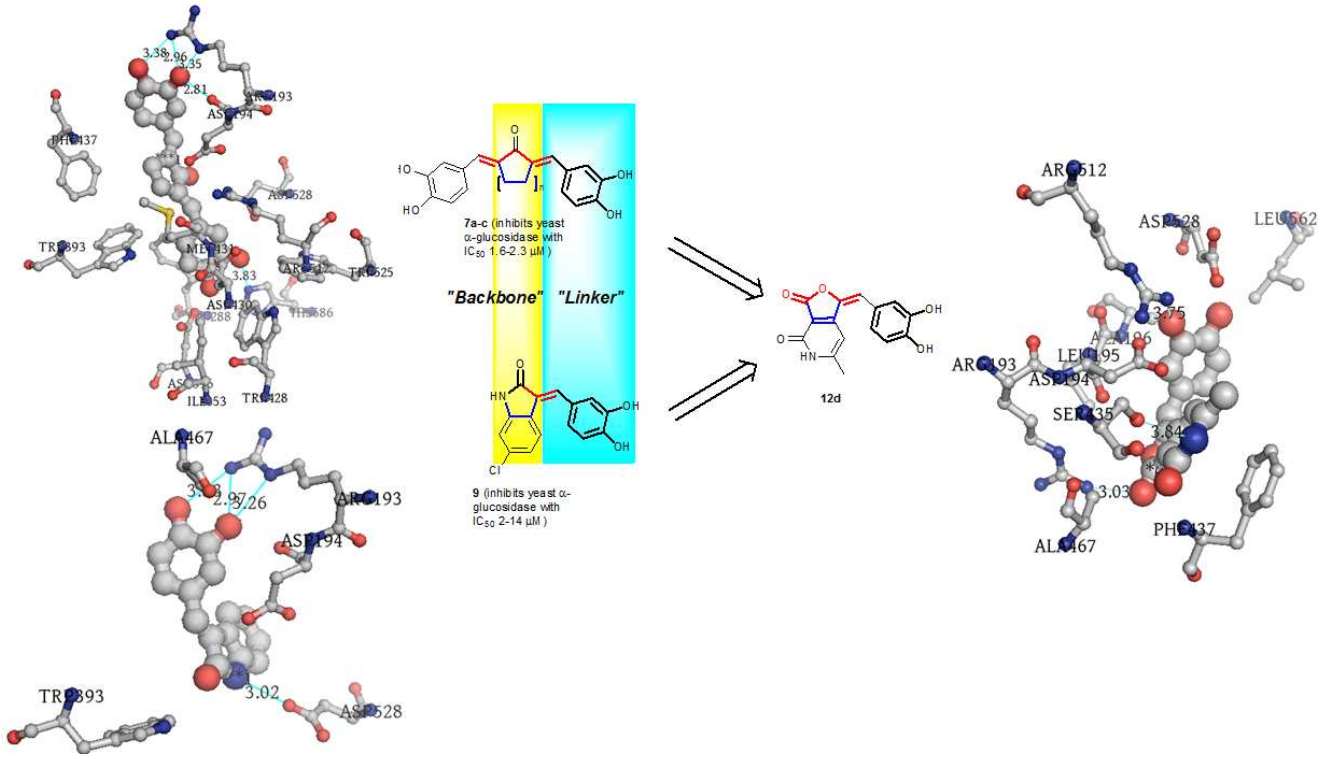

Figure 2. Design of the furopyridinedione molecules (**12a-v**) from scaffold hopping and bioisosteric substitution of **7a** and **9a**

Results and discussion

Chemistry

The target library (**12a-v**) was synthesized as depicted in scheme 1. The reaction involved, aldol condensation of furopyridinedione **13** and appropriate aldehydes (**14a-p** and **15a-f**) in presence piperidine as base and in ethanol under refluxing condition (80-90°C). The final compounds precipitated during the course of the reaction and they were filtered and washed with hexane for purification. They were characterized by routine ^{1}H, ^{13}C and LCMS. For the aromatic substituents, in general the yields of the final molecules with electron withdrawing functionalities (**12c**, **h** and **l**) are better (70-92%) compared to their electron donating counterpart *viz.* **12a**, **b**, **d-f**, **g**, **i-k** (35-72%). Additionally the heteroaromatic aldehydes afforded the desired compounds (**12l-p**) in moderate yield (62-75%). The 4-subitituted thiophene analogs (**12q-v**) were synthesized from aldehydes **15a-f**. Aldehydes **15a-e** were synthesized by Suzuki coupling of 4-bromothiophene-2-carbaldehyde with phenyl, 3-pyridyl, 2-methoxy-5-pyridyl, 2-(N-Boc-N-piperizinyl)-5-pyridyl, 4-fluorostyryl- boronic acids, catalytic palladium bis triphenyl phosphine chloride, sodium carbonate (as base) and dimethyl formamide (DMF) (as solvent) at 110°C. Aromatic nucleophilic substitution (S_NAr) of 4-bromothiophene-2-carbaldehyde with piperidine afforded **15f**.

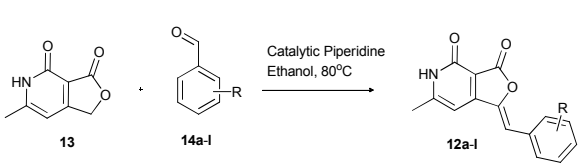

Aldehydes	Compound #	R	Yield (%)
14a	**12a**	2,4-dimethyl	47
14b	**12b**	4-methoxy-2,3-dimethy	54
14c	**12c**	2-trifluoromethyl	72
14d	**12d**	3,4-dihydroxy	35
14e	**12e**	3-bromo	51
14f	**12f**	4-bromo	59
14g	**12g**	3-naphthalyl	74
14h	**12h**	3,4-difluoro	85
14i	**12i**	3-[1,3-dioxole]	48
14j	**12j**	2,3-dimethox	64
14k	**12k**	H	71
14l	**12l**	4-nitro	92

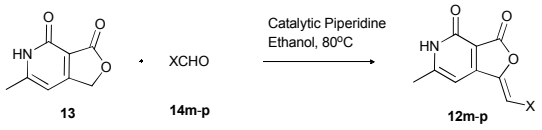

Aldehydes	Compound #	X	Yield (%)
14m	**12m**	3-indolyl	71
14n	**12n**	2-N-methylimidazolyl	68
14o	**12o**	2-thiophenyl	72
14p	**12p**	4-bromo-2-thiophenyl	65

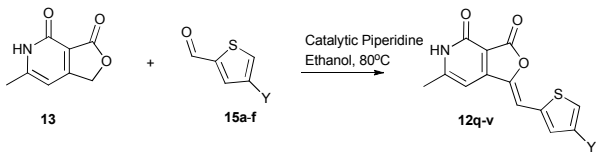

Aldehydes	Compound #	Ar	Yield (%)
15a	**12q**	Phenyll	49
15b	**12r**	3-pyridyl	34
15c	**12s**	2-methoxy-3-pyridyl	51
15d	**12t**	2-(N-Boc-N-piperazinyl-3-pyridyl	43
15e	**12u**	4-fluorostyryl	36
15f	**12v**	Piperidine	71

Scheme 1. Synthesis of the library molecules **12a-v**

In general the ^{1}H-spectra of all the final compounds (**12a-v)** are characterized by a singlet at ~2.3ppm that corresponds to the methyl (CH_3) on the pyridone moiety and are heavy at the aromatic region between 6.5-8.8 ppm. For compound **12t** the densely congregated peaks at the aliphatic region (3-4 ppm) can be attributed to the piperizinyl moiety. Similarly the peak at 1.7 and at 4 ppm in **12v** is because of the piperidine ring. In general the ^{13}C spectra of these compounds are characterized by the amide and lactone carbonyl at 165 and 160 ppm respectively.

Pharmacological study

α-glucosidase inhibition

The library of aryl and heteroaryl furopyridine diones were screened against α-glucosidase (yeast origin) with acarbose as reference inhibitor. 100 µL of nitrophenol-D-glucopyranoside substrate (2mM PNP-Glc dissolved in 2mM phosphate buffer at pH of 7.2) (actual substrate concentration was 0.31mgmL^{-1} to 0.93 mgmL^{-1}) along with the test compounds at concentrations ranging from 0.1-1 µM and 10-50 µM were taken in 96 well plates. Next the final volume of reaction mixture was made to 200 µL with 2 mM phosphate buffer (pH 7.2). The hydrolytic reaction commenced by the addition of α-glucosidase enzyme (0.5 m/mL) and the plates were incubated at 37°C for 15 minutes. Finally, the reaction was terminated by adding 50 µL of 2N Na_2CO_3. To know the potency of the test compounds, the percentage inhibitions observed were plotted against the concentration using non-linear regression approach (data not shown) from which the IC_{50} concentrations were computed.

Table 1. α-glucosidase inhibition of **12a-v**

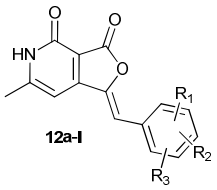

12a-l

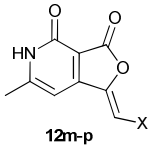

12m-p

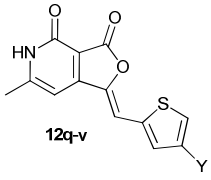

12q-v

Entry	R_1	R_2	R_3	X	Y	α-glucosidase IC_{50} (µM)
12a	2-Me	5-Me	-	-	-	NA

12b	2-Me	3-Me	4-OMe	-	-	NA
12c	2-CF_3	-	-	-	-	23 ± 0.12
12d	3-OH	4-OH	-	-	-	2 ± 0.02
12e	3-Br	-	-	-	-	41 ± 0.21
12f	4-Br	-	-	-	-	10 ± 0.63
12g	2-Napthalyl	-	-	-	-	NA
12h	3-F	4-F	-	-	-	1 ± 0.09
12i	3,4-(O-CH_2-O)					NA
12j	2-OMe	3-OMe	-	-	-	NA
12k	H	-	-	-	-	53 ± 0.38
12l	2-NO_2	-	-	-	-	3.4 ± 0.55
12m	-	-	-	2-indolyl	-	2 ± 0.15
12n	-	-	-	N-Me-2-imidazolyl		0.9 ± 0.04
12o	-	-	-	2-thiophenyl	-	10 ± 0.30
12p	-	-	-	4-bromo-2-thiophenyl	-	0.24 ± 0.04
12q	-	-	-	-	Phenyl	8.3 ± 0.39
12r	-	-	-	-	3-pyridyl	NA
12s	-	-	-	-	2-OMe-3-pyridyl	30 ± 0.60
12t	-	-	-	-	N-Boc-2-piperizinyl-3-pyridyl	86 ± 0.62
12u	-	-	-	-	4-fluorostyryl	NA
12v	-	-	-	-	N-piperidinyl	NA
Acarbose	-	-	-	-	-	17 ± 0.7

Note: (1) NA: No activity was observed; (2) IC_{50}: Concentration of inhibition required for half-maximal enzyme inhibition and is reported as means of two independent experiments; (3) The screening assays for finding these IC_{50} concentrations were performed at pH 7.0, temperature 37°C

Structure activity relationship

Based on the results obtained from the α-glucosidase inhibitory activity of the molecules (**12a-v**), we segregated the library into three segments (Figure 3). Segment 1, contained the furopyridinedione attached to diversely substituted aromatic groups, segment 2, with various heteroaromatic group and segment 3, with substituted thiophenes. Assessment of these segments illustrated evolution of the initial structure activity relationship studies that direct toward the lead structure with improved inhibitory activity.

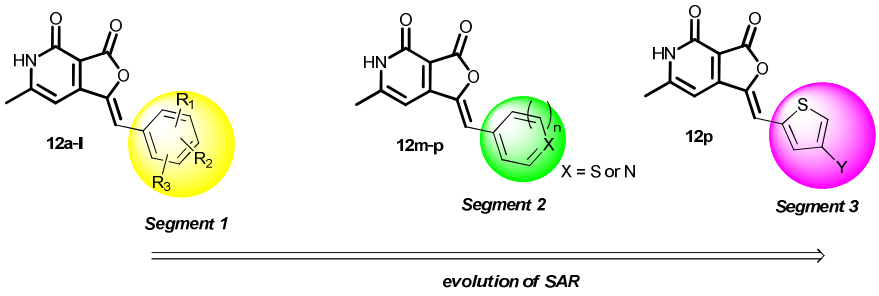

Figure 3. Structure activity relationship studies

The activity results in table 1 indicated that quite a few molecules in the library such as **12 d**, **f**, **h**, **l**, **m**, **n**, **p**, and **q** are more active than the reference molecule acarbose (17.4 μM). Interestingly the substitution pattern in segment 1, significantly influenced the activity of the compound, where compounds with electron withdrawing substituents such as **12c**, **f**, **h** and **l** are significantly more potent (IC_{50} range 1→21 μM) than their electron donating analogs (IC_{50} range 40→54 μM). In general the segment 2 compounds are more active than segment 1. Among them compound **12p** is the lead candidate exhibiting inhibition with an IC_{50} of 0.24 μM. It contained a thiophene ring, substituted with bromide at C_4. The chemical reactivity of the bromide in **12p** is a concern, however it is too early to comment on that. Especially when there is abundant bromide containing drugs in the market such as, vasodilator nicergoline, the sedative brotizolam, the anticancer agent pipobroman, antiseptic merbromin and etc.[20] The N-methyl imidazole substituted **12n** is another promising compound with an IC_{50} of 0.89 ± 0.007 μM. It is noteworthy that further modification of the C_4 bromide of **12p** with aryl, alkenyl, heteroaryl and 2°-amines (**12q-v**) could not improve the activity profile any further. This indicates a very tight SAR in this region which requires subtle substitutions to improve the activity. Additionally screening of **12p** against mammalian COS cell lines indicated it to be nontoxic (refer *SI*).

Reaction kinetics study

Inhibitory kinetic assays were performed to identify the mode of inhibition of the highest effective molecule, **12p** over α-glucosidase. The study was executed by graphical means of employing primary (Lineweaver-Burk) and secondary plots.[21] Fig. 4 illustrates the α-glucosidase inhibition kinetic plots and it can be observed that all the data lines on the Lineweaver-Burk plots of **12p** intersected in the second quadrant indicating a mixed type of inhibition over α-glucosidase enzyme. The inhibition mechanism, indeed, involved the binding of this inhibitor to both glucosidase and the glucosidase + substrate complex.[22] There is a possibility that **12p** binds to an allosteric site of the enzyme, α-glucosidase (yeast origin) and the substrate is bound to its active site. Mixed type of inhibition subsidizes two inhibition constants *viz*. K_1 and K_2 (the observed K_m for the employed substrate concentration was 0.53 mg/mL). The constants were determined from the slope of 2° plots and Y-intercepts from LB-plot against the concentration of each inhibitor (data not shown in this paper). Hence for **12p**, the K_1 and K_2 constants with α-glucosidase were computed as 0.22 ±0.008 µM and 0.25 ± 0.002 µM. The smaller dissociation constants indicated stronger inhibition by the enzymes.

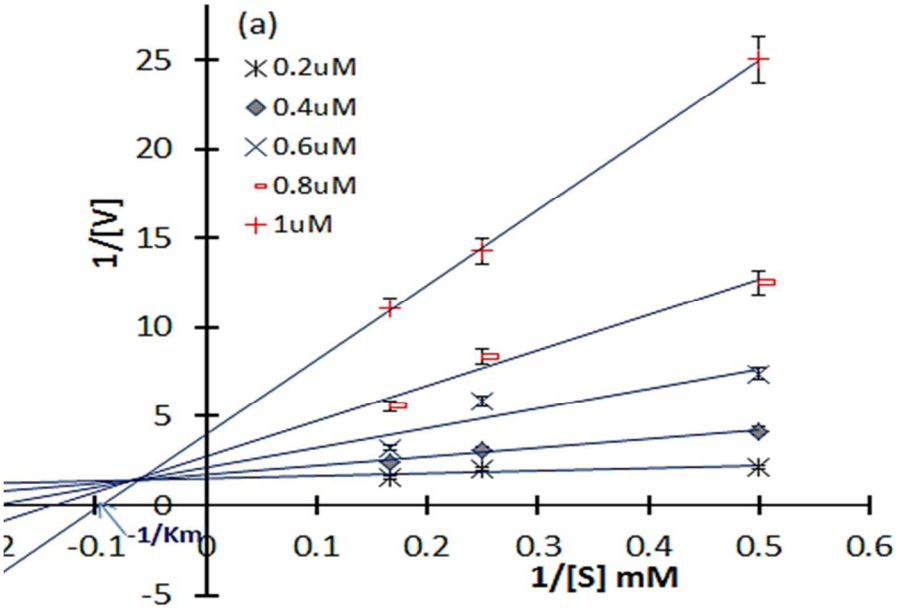

Figure 4. Double-reciprocal (Lineweaver-Burk) plots of α-glucosidase (yeast) inhibition kinetics exhibited by compound **12p**; α-Glucosidase (0.5IU/mL) was exposed to **12p** at 37ºC for 10min, followed by varying concentrations of 4-nitrophenyl α-D-glucopyranoside (PNPG).

X-ray crystallography

In order to confirm the conformation of compound **12p** we determined its three dimensional structure *via* single-crystal X-ray diffraction experiment. The compound **12p** was crystallized at room temperature by slow evaporation of its solution in *N*-methyl-2-pyrrolidone (NMP). Interestingly the X-ray structure revealed that the compound **12p** has co-crystallized with NMP, essentially due to the presence of a strong N-H…O hydrogen bond between the N-H of compound **12p** and O=C of NMP (Figure 5). Both compound **12p** and the solvent NMP are in planar geometry and they found to be lying almost in the same plane. Both the molecules together packs in the crystal lattice in an anti-parallel fashion and form a zig-zag pattern (Figure 6). In the crystal structure, the strong intermolecular N-H…O hydrogen bond and $\pi\ldots\pi$ stacking with short inter-planar distance of about 3.5 Å lead to the formation of three dimensional framework. Crystallization experiment with other solvents and the search of a crystal structure with only compound **12p** molecule is in progress.

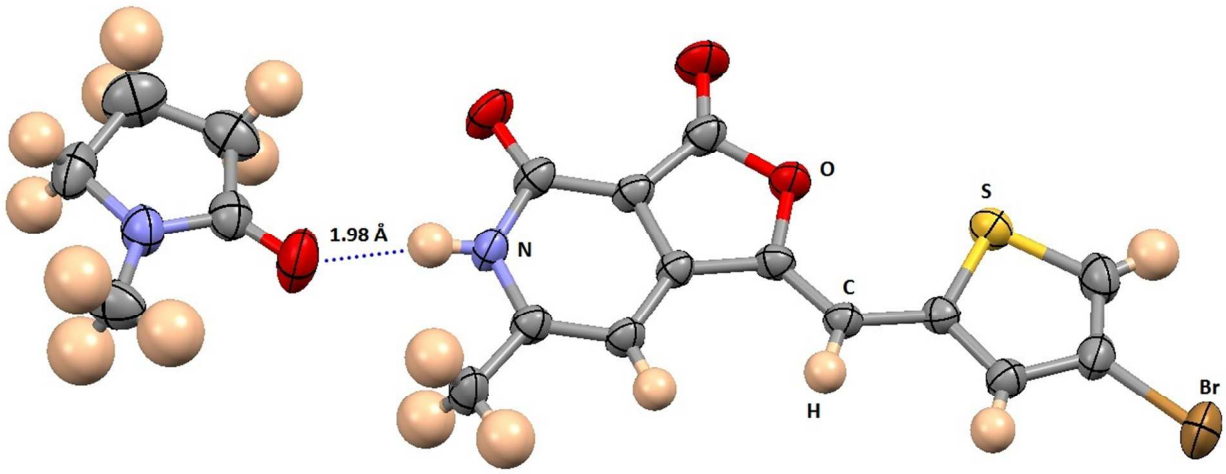

Figure 5: ORTEP diagram of compound **12p** co-crystallized with *N*-methyl-2-pyrrolidone (NMP). Ellipsoids of non-hydrogen atoms are drawn at 50% probability level. The color codes of different atom types are shown in the figure. The N-H…O hydrogen bond between **12p** and NMP is shown as blue dotted line.

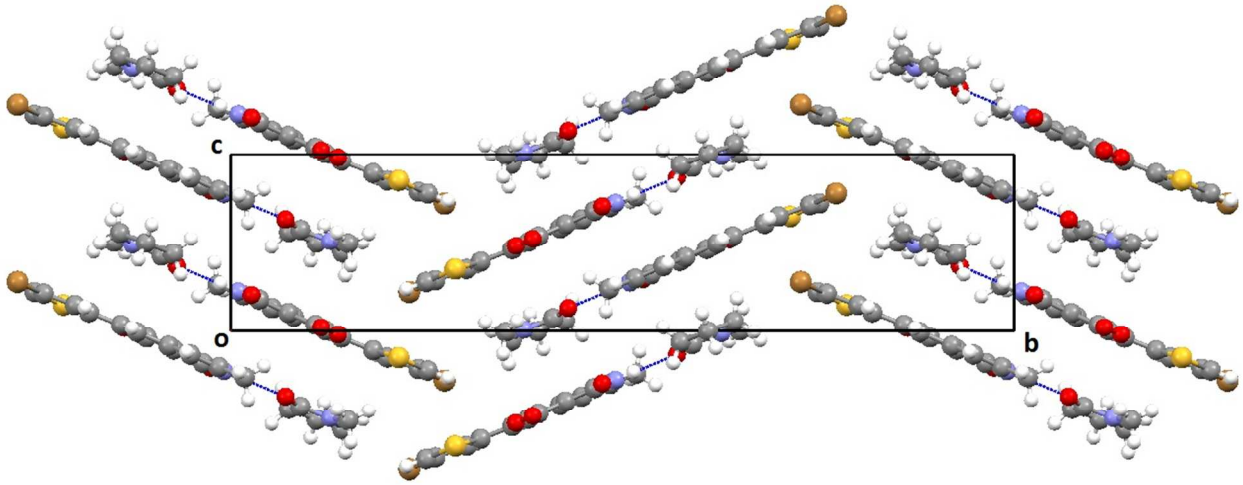

Figure 6: Packing diagram of **12p**-NMP complex viewed down the *a*-axis showing the molecular arrangement in the crystal structure and the unique N-H…O hydrogen bond between **12p** and NMP, shown as blue dotted line.

Docking experiments of 12p

Molecular docking of 12p

To understand the binding interaction of **12p** and acarbose with α-glucosidase the molecular docking was conducted against the homology model of α-glucosidase. After docking we received two alpha-glucosidase co12p and acarbose binding to the active site of modelled α-glucosidase protein by forming various bonded and non-bonded interactions. **12p** is bonded to α-glucosidase with predicted binding energy -6.24 kcal/mol while acarbose binds to α-glucosidase with predicted binding energy of -4.45 kcal/mol.

Our predicted binding model suggests that **12p** formed two hydrogen bonds with ASP194 and SER588 residues *via* the nitrogen of the pyridine moiety and the sulphur of the thiophene moiety respectively, while sharing non-bonded interaction with TRP393, MET431, ASP528, PHE561, LEU562, LEU589, LEU590 (Figure 7a).

Acarbose formed hydrogen bonds with ASP194, SER 435, ASN436, ALA467, SER591, GLY563, LEU589 and LEU590 residues while sharing non-hydrogen bonds interaction with TRP288, TRP393, MET431, TRP530 and LEU562 (Figure 7b).

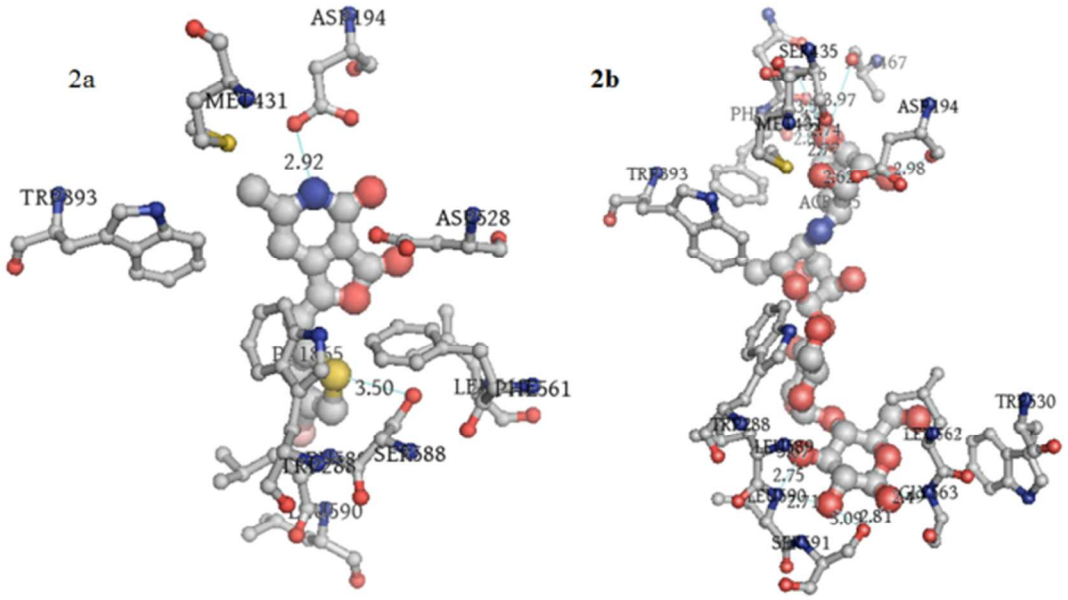

Figure 7. (a) 3D representation of interaction between **12p** with alpha-glucosidase modelled protein. (b) 3D representation of interaction between acarbose and alpha-glucosidase modelled protein

Molecular dynamic simulation

MD simulations were performed for alpha-glucosidase-**12p** complex by Desmond 3.2 software, using OPLS_2005 force field for 47 ns simulation time. The protein-ligand complex was solvated in a 10 × 10 × 10 Å orthorhombic box with periodic boundary conditions by adding TIP3P water molecules. The whole system was neutralized by adding ions Na+ and Cl− so that the net charge of the system becomes 0. Herein we used the default protocol of desmond for relaxing the model. After default relaxation which includes various restrained and without restrained minimization, the model is further relaxed using NPT (number of atom, pressure, and temperature) ensemble class at temperature 300K and pressure 1.01325 bar. Long-range electrostatic interactions were computed using particle-mesh Ewald method and van der waals (VDW) cut-off was set to 9 Å. The SHAKE algorithm was used to satisfy the hydrogen bond geometry constraints during simulation.

MD simulation helps in identifying the structural stability and flexibility present in the protein structure with time. It also helps in identifying the dynamic properties of the protein ligand complex. Simulation quality analysis plot showed that various parameters like total energy,

potential energy, temperature, pressure and volume were relatively stable throughout our MD simulation (Figure 8a). RMSD plot for protein backbone and heavy atoms showed initial rearrangement but attained stability after 10 ns of simulation (Figure 8b). Same is observed in case of Ligand RMSD (Figure 9b).The backbone and heavy atoms of α-glucosidase showed a RMSD of range 1- 2.6 Å and 1.2 – 3.2 Å respectively. By analysing the root mean square fluctuation (RMSF) plot, we can say that most of the residues were within the limit of 2.5 Å. Some residues which were present in the loop of the protein exceeded 2.5 Å (Figure 8c). Protein secondary structure elements (SSE) like alpha-helices and beta-strands were monitored throughout the simulation and no major conformational changes in SSE were observed (Figure 8d). RMSD plot, RMSF plot, SSE plot and energy plot revealed that α-glucosidase-**12p** complex were stable throughout the simulation.

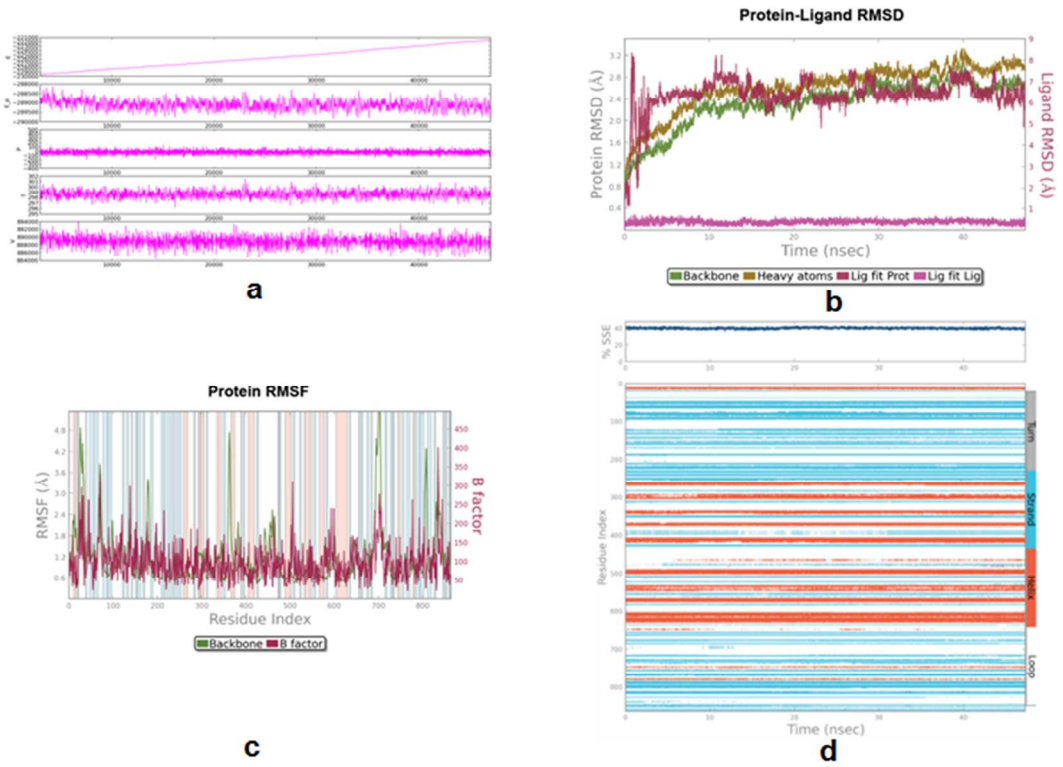

Figure 8. a) Simulation Quality plot of MD simulation of alpha-glucosidase-8 complex during 47ns simulation. This plot showing the total energy, potential energy, pressure, temperature and volume observed during the simulation period. b) RMSD plot of protein-ligand complex during simulation. c) RMSF plot of protein-ligand complex during simulation. d) Secondary Structure elements (SSE) plot of protein during simulation.

All the bonded and non-bonded interaction between **12p** and α-glucosidase were monitored throughout the simulation. The overall interactions between **12p** and α-glucosidase were shown in (Figure 9a). After 47 ns simulations the final structure of α-glucosidase-**12p** complex along with their binding interactions are depicted in Figure 9b. Throughout the simulation major interaction between **12p** and α–glucosidase are: H-bond interaction with ASP316, SER588 and LEU 589 residues while hydrophobic interaction are with TRP 288, LEU 317, ILE353, PHE561, ARG584 and HIS586 residues. Water bridges were present with ARG287, HIS586, SER588, and LEU589.

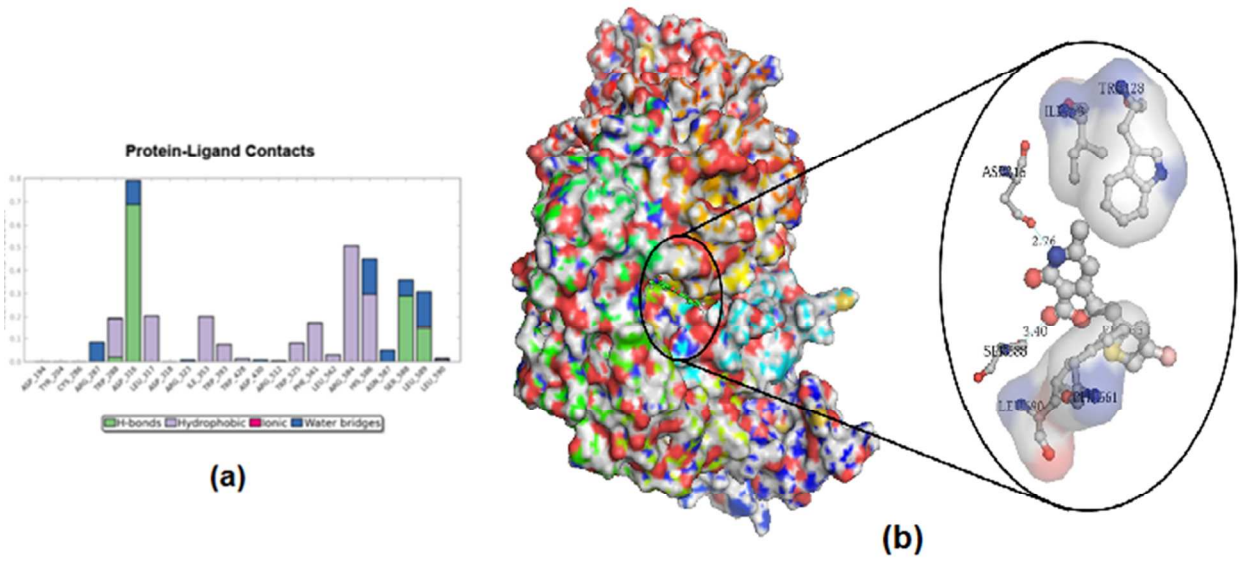

Figure 9. (a) Interaction plot of protein-ligand complex during simulation. (b) Interaction of **12p** with α-glucosidase after 47 ns simulation

Conclusion

Hence, to generate a novel molecule against α-glucosidase, a small molecule library of 22 furopyridinediones was designed using an intuitive scaffold hopping and bioisosteric modification of few existing α-glucosidase inhibitors. They were synthesized *via* an aldol condensation reaction and the structures were confirmed based on NMR spectroscopy, mass analysis and single crystal X-ray crystallography of **12p**. This library was further screened against α-glucosidase (yeast origin) with acarbose as the positive standard. Among the assayed compounds, **12p** emerged as the most potent candidate showing inhibition with IC_{50} value of 0.24 μM, which is 100 fold more active than the reference compound. This compound

incorporated a bromide at the C_4 position of a thiophene moiety which in turn was connected to the furopyridinedione at C_2 via a methylene linkage. Reaction kinetics revealed it to be a mixed inhibitor. Molecular modelling and molecular dynamic simulation experiments revealed potential putative binding pockets of **12p** along with the active region of α-glucosidase. This inhibitor can be considered as a favorable lead towards further investigation of an antidiabetic molecule.

Experimental

General

All reactions were carried out in flame-dried sealed tubes with magnetic stirring. Unless otherwise noted, all experiments were performed under argon atmosphere. All reagents were purchased from Sigma Aldrich, Acros or Alfa Aesar. Solvents were treated with 4 Å molecular sieves or sodium and distilled prior to use. Purifications of reaction products were carried out by column chromatography using Chem Lab silica gel (230-400 mesh). Infrared spectra (IR) were recorded on a Thermoscientific Neoled IS5 FTIR spectrophotometer and are reported as wavelength numbers (cm^{-1}). Infrared spectra were recorded by preparing a KBr pellet containing the title compound. ^1H NMR and ^{13}C NMR spectra were recorded with tetramethylsilane (TMS) as internal standard at ambient temperature unless otherwise indicated on a Varian 300/400 and JEOL JNM-ECX500 MHz at 500 MHz for ^1H NMR and 100 MHz for ^{13}C NMR. Chemical shifts are reported in parts per million (ppm) and coupling constants are reported as Hertz (Hz). Splitting patterns are designated as singlet (s), broad singlet (bs), doublet (d), triplet (t). Splitting patterns that could not be interpreted or easily visualized are designated as multiple (m). The Mass Spectrometry analysis was done on the 6540 UHD Accurate-Mass Q-TOF LC/MS system (Agilent Technologies) equipped with Agilent 1290 LC system obtained by the Dept. of Chemistry, School of Natural Sciences, Shiv Nadar University, Uttar Pradesh 203207, India.

General procedure for the aldol condensation between 6-methylfuro[3, 4-c]pyridine-3, 4(1H,5H)-dione and appropriate aldehydes

To a stirred solution of 6-methylfuro[3,4-c]pyridine-3,4(1H,5H)-dione (300 mg, 1.8 mmoles) in ethanol (10 mL) added piperidine (15 mg, 0.18 mmol), followed by corresponding aldehyde (1.98 mmoles) under N_2 atmosphere at room temperature, then the reaction mixture stirred at 80°

C for 16 h, allowed to cool to room temperature added diethyl ether (10 mL) the resulting precipitate was collected by filtration, washed with diethyl ether (3 × 10 mL), and dried to give substituted 6-methylfuro[3,4-c]pyridine-3,4(1H,5H)- dione.

(Z)-1-(2,4-dimethylbenzylidene)-6-methylfuro[3, 4-c]pyridine-3, 4(1H,5H)-dione (**12a**)

Following the general protocol 2, 4-dimethylbenzaldehyde (267 mg, 1.98 mmoles) afforded **12a** in 238 mg (yield 47%). ^{1}H NMR (300 MHz; DMSO-d_6): δ 12.21 (br. s, 1H), 7.81 (m, 1H), 7.23-7.19 (m, 1H); 7.17-7.15 (m, 1H); 6.98-6.85 (m, 2H), 2.36 (s, 3H), 2.35-2.34 (m, 6H). ^{13}C NMR (125 MHz; DMSO-d_6): δ 164.84, 157.98, 156.65, 155.67, 143.16, 135.61, 135.39, 131.38, 130.95, 130.52, 109.28, 106.01, 97.79, 21.15, 19.92, 19.72. LCMS (ESI) m/z: $[M + H]^+$ calculated for ($C_{17}H_{16}NO_3$) 282.11, found 282.27.

(Z)-1-(4-methoxy-2,3-dimethylbenzylidene)-6-methylfuro[3,4-c]pyridine-3,4(1H,5H)-dione (**12b**)

Following the general protocol 4-methoxy-2, 3-dimethylbenzaldehyde (324 mg, 1.98 mmoles) afforded **12b** in 303 mg (yield 54%). ^{1}H NMR (300 MHz; DMSO-d_6): δ 12.15 (br. s, 1H), 7.85-7.83 (d, *J* = 6 Hz, 1H), 7.01-6.95 (m, 3H); 3.81 (s, 3H), 2.27-2.26 (d, J = 3Hz, 6H), 2.18 (s, 3H). ^{13}C NMR (125 MHz; DMSO-d_6): δ 164.90, 158.29, 156.71, 155.11, 141.76, 138.47, 129.06, 124.98, 123.96, 110.47, 108.88, 105.45, 97.42, 56.04, 20.38, 16.39, 12.32. LCMS (ESI) m/z: $[M + H]^+$ calculated for ($C_{18}H_{19}NO_4$) 312.58, found 312.25.

(Z)-1-(2-trifluoromethylbenzylidene)-6-methylfuro[3,4-c]pyridine-3,4(1H,5H)-dione (**12c**)

Following the general protocol 2-trifluoromethylbenzaldehyde (345 mg, 1.98 mmoles) afforded **12c** in 416 mg (yield 72%). ^{1}H NMR (300 MHz; DMSO-d_6): δ 11.99-11.80 (br. s, 1H), 8.20-8.18 (d, *J* = 6 Hz, 1H), 7.86-7.78 (m, 2H), 7.61-6.58 (m, 1H), 6.85 (s, 1H), 6.80 (s, 1H), 2.34 (s, 3H). ^{13}C NMR (125 MHz; DMSO-d_6): δ 164.19, 157.98, 157.02, 156.09, 145.45, 133.29, 132.57, 130.64, 129.69, 127.56, 127.31, 126.64, 106.59, 105.27, 97.52, 19.96. LCMS (ESI) m/z: $[M + H]^+$ calculated for ($C_{16}H_{11}F_3NO_3$) 322.06, found 322.00.

(Z)-1-(3,4-dihydroxybenzylidene)-6-methylfuro[3,4-c]pyridine-3,4(1H,5H)-dione (**12d**)

Following the general protocol 3,4-dihydroxybenzaldehyde (273 mg, 1.98 mmoles) afforded **12d** in 180 mg (yield 35%). ^{1}H NMR (300 MHz; DMSO-d_6): δ 7.39 (s, 1H), 7.16-7.05 (m, 1H), 6.80-6.75 (m, 2H), 6.72 (s, 1H), 2.28 (s, 3H). ^{13}C NMR (125 MHz; DMSO-d_6): δ 168.75, 167.43, 164.90, 158.35, 156.71, 155.05, 148.29, 146.05, 140.58, 124.67, 124.40, 117.66, 116.45, 113.39, 109.28, 105.14, 99.84, 97.03, 68.28, 20.00, 19.65. LCMS (ESI) m/z: $[M + H]^+$ calculated for ($C_{15}H_{12}NO_5$) 286.06, found 286.00.

(Z)-1-(3-bromobenzylidene)-6-methylfuro[3,4-c]pyridine-3,4(1H,5H)-dione (**12e**)

Following the general protocol 3-bromobenzaldehyde (364 mg, 1.98 mmoles) afforded **12e** in 305 mg (yield 51%). ^{1}H NMR (300 MHz; DMSO-d_6): δ 12.41-12.21 (bs, 1H), 8.00 (s, 1H), 7.80-7.75 (d, J = 15 Hz, 1H), 7.61-7.56 (m, 1H), 7.48-7.40 (m, 1H), 6.99 (s, 1H), 6.68 (s, 1H), 2.31 (s, 3H). ^{13}C NMR (125 MHz; DMSO-d_6): δ 168.30, 158.04, 156.54, 156.27, 144.10, 135.53, 132.74, 132.23, 131.52, 129.71, 122.61, 109.86, 106.10, 97.35, 56.50, 20.10, 19.01. LCMS (ESI) m/z: $[M + H]^+$ calculated for ($C_{15}H_{11}BrNO_3$) 332.1488, found 332.0950.

(Z)-1-(4-bromobenzylidene)-6-methylfuro[3,4-c]pyridine-3,4(1H,5H)-dione (**12f**)

Following the general protocol 4-bromobenzaldehyde (364 mg, 1.98 mmoles) afforded **12f** in 355 mg (yield 59%). ^{1}H NMR (300 MHz; DMSO-d_6): δ 12.35-12.25 (bs, 1H), 7.79-7.81 (m, 4H), 6.98 (s, 1H), 6.67 (s, 1H), 2.36 (s, 3H). ^{13}C NMR (125 MHz; DMSO-d_6): δ 164.37, 158.10, 156.61, 156.11, 143.67, 132.58, 132.49, 132.44, 123.18, 110.45, 106.02, 97.34, 20.09. LCMS (ESI) m/z: $[M + H]^+$ calculated for ($C_{15}H_{11}BrNO_3$) 332.1488, found 332.1330.

(Z)-6-methyl-1-(naphthalen-2-ylmethylene)furo[3,4-c]pyridine-3,4(1H,5H)-dione (**12g**)

Following the general protocol 3-naphthaldehyde (311 mg, 1.98 mmoles) afforded **12g** in 404 mg (yield 74%). ^{1}H NMR (300 MHz; DMSO-d_6): δ 12.23 (bs, 1H), 8.59-8.42 (m, 1H), 8.25-8.19 (m, 1H), 8.01-7.95 (m, 2H), 7.65-7.52 (m, 4H), 7.19 (s, 1H), 2.36 (s, 3H). ^{13}C NMR (125 MHz; DMSO-d_6): δ 164.75, 158.31, 156.75, 155.92, 144.54, 133.84, 131.77, 130.29, 130.24, 129.77, 129.11, 127.42, 126.87, 126.17, 124.32, 107.50, 105.94, 97.93, 20.17. LCMS (ESI) m/z: $[M + H]^+$ calculated for ($C_{19}H_{14}NO_3$) 304.09, found 304.23.

(Z)-1-(3, 4-difluorobenzylidene)-6-methylfuro[3,4-c]pyridine-3,4(1H,5H)-dione (**12h**)

Following the general protocol 3,4-difluorobenzaldehyde (281 mg, 1.98 mmoles) afforded **12h** in 442 mg (yield 85%). ^{1}H NMR (300 MHz; DMSO-d_6): δ 12.25 (bs, 1H), 7.85-7.79 (m, 1H), 7.62-7.55 (m, 2H), 6.99 (s, 1H), 6.62 (s, 1H), 2.34 (s, 3H). ^{13}C NMR (125 MHz; DMSO-d_6): δ 164.21, 158.00, 156.47, 156.26, 143.69, 130.88, 128.11, 118.99, 118.85, 118.76, 118.62, 109.32, 106.00, 97.23, 20.07. LCMS (ESI) m/z: $[M + H]^+$ calculated for ($C_{15}H_{10}F_2NO_3$) 290.05, found 290.17.

(Z)-1-(benzo[d][1,3]dioxol-5-ylmethylene)-6-methylfuro[3,4-c]pyridine-3,4(1H,5H)-dione (**12i**)

Following the general protocol benzo[d][1,3]dioxole-5-carbaldehyde (300 mg, 1.98 mmoles) afforded **12i** in 256 mg (yield 48%). ^{1}H NMR (300 MHz; DMSO-d_6): δ 12.18 (bs, 1H), 7.40 (s, 1H), 7.35-7.33 (d, J = 6 Hz, 1H), 7.10-7.05 (m, 1H), 6.89 (s, 1H), 6.64-6.63 (d, J = 3 Hz, 1H), 6..05 (s, 2H), 2.34 (s, 3H). ^{13}C NMR (125 MHz; DMSO-d_6): δ 164.55, 158.19, 156.64, 155.50, 148.90, 148.33, 141.64, 127.38, 126.64, 112.13, 109.73, 109.39, 105.50, 102.18, 97.05, 20.02. LCMS (ESI) m/z: $[M + H]^+$ calculated for ($C_{16}H_{12}NO_5$) 298.06, found 298.18.

(Z)-1-(2,3-dimethoxybenzylidene)-6-methylfuro[3,4-c]pyridine-3,4(1H,5H)-dione (**12j**)

Following the general protocol 2,3-dimethoxybenzaldehyde (328 mg, 1.98 mmoles) afforded **12j** in 362 mg (yield 64%). ^{1}H NMR (300 MHz; DMSO-d_6): δ 12.20 (bs, 1H), 7.40 (s, 1H), 7.64-7.62 (m, 1H), 7.21-7.15 (m, 2H), 6.95 (s, 1H), 6.88 (s, 1H) 3.80 (s, 6H), 2.31)s, 1H). LCMS (ESI) m/z: $[M + H]^+$ calculated for ($C_{15}H_{12}NO_5$) 314.09, found 314.21.

(Z)-1-benzylidene-6-methylfuro[3,4-c]pyridine-3,4(1H,5H)-dione (**12k**)

Following the general protocol benzaldehyde (210 mg, 1.98 mmoles) afforded **12k** in 321 mg (yield 74%). ^{1}H NMR (500 MHz; DMSO-d_6): δ 12.00 (br. s, 1H), 7.82-7.78 (m, 2H), 7.59-7.39 (m, 3H), 6.99 (s, 1H); 6.79 (s, 1H), 2.31 (s, 3H). ^{13}C NMR (125 MHz; DMSO-d_6): δ 164.59, 158.17, 156.78, 155.94, 143.19, 133.21, 130.86, 129.83, 129.49, 111.82, 105.95, 97.34, 20.20. LCMS (ESI) m/z: $[M + H]^+$ calculated for ($C_{15}H_{12}NO_3$) 254.07, found 254.14.

(Z)-6-methyl-1-(4-nitrobenzylidene)furo[3,4-c]pyridine-3,4(1H,5H)-dione (**12l**)

Following the general protocol 4-nitrobenzaldehyde (300 mg, 1.98 mmoles) afforded **12l** in 493 mg (yield 48%). ^{1}H NMR (500 MHz; DMSO-d_6): δ 12.36 (br. s, 1H), 8.35 (d, 2H, J = 5 Hz), 8.015 (d, 2H, J = 5 Hz); 7.12 (s, 1H); 6.81 (s, 1H), 2.35 (s, 3H). ^{13}C NMR (125 MHz; DMSO-

d_6): δ 166.60, 162.39, 161.43, 160.24, 146.85, 143.08, 130.95, 128.02, 128.02, 124.15, 124.15, 119.95, 22.55. HRMS (ESI-TOF) m/z: $[M + H]^+$ calculated for ($C_{15}H_{11}N_2O_5$) 299.0662, found 299.0662.

(Z)-1-((1H-indol-3-yl)methylene)-6-methylfuro[3,4-c]pyridine-3,4(1H,5H)-dione (**12m**)

Following the general protocol 1H-indole-3-carbaldehyde (290 mg, 1.98 mmoles) afforded **12m** in 374 mg (yield 71%). ^{1}H NMR (500 MHz; DMSO-d_6): δ 11.99 (br. s, 1H), 8.01 (m, 2H), 7.31-7.25 (m, 1H); 7.39 (s, 1H); 7.21-7.18 (m, 3H), 6.82 (s, 1H), 2.39 (s, 3H). ^{13}C NMR (125 MHz; DMSO-d_6): δ 168.77, 167.41, 164.88, 158.56, 158.38, 155.79, 155.05, 154.35, 139.38, 136.44, 130.69, 126.96, 123.02, 121.01, 119.26, 112.72, 109.59, 109.29, 106.85, 104.80, 99.84, 96.94, 68.29, 19.99, 19.65. LCMS (ESI) m/z: $[M + H]^+$ calculated for ($C_{17}H_{13}N_2O_3$) 293.08, found 293.00.

(Z)-6-methyl-1-((1-methyl-1H-imidazol-4-yl)methylene)furo[3,4-c]pyridine-3,4(1H,5H)-dione (**2n**)

Following the general protocol 1-methyl-1H-imidazole-4-carbaldehyde (218 mg, 1.98 mmoles) afforded **12n** in 315 mg (yield 68%). ^{1}H NMR (500 MHz; DMSO-d_6): δ 11.98 (br. s, 1H), 8.03 (m, 1H), 7.61-7.55 (m, 1H); 7.49 (s, 1H); 6.86 (s, 1H), 3.92 (s, 3H), 2.31 (s, 3H). ^{13}C NMR (125 MHz; DMSO-d_6): δ 164.36, 158.08, 155.29, 153.91, 138.86, 136.50, 133.84, 127.01, 122.71, 120.83, 118.90, 110.64, 108.20, 105.93, 96.48. LCMS (ESI) m/z: $[M + H]^+$ calculated for ($C_{13}H_{12}N_3O_3$) 258.08, found 258.19.

(Z)-6-methyl-1-(thiophen-2-ylmethylene)furo[3,4-c]pyridine-3,4(1H,5H)-dione (**12o**)

Following the general protocol thiophene-2-carbaldehyde (232 mg, 1.98 mmoles) afforded **12o** in 325 mg (yield 72%). ^{1}H NMR (400 MHz; DMSO-d_6): δ 12.17 (br. s, 1H), 7.86 (s, 1H), 7.47-7.19 (t, 3H); 6.71 (s, 1H); 2.32 (s, 3H). ^{13}C NMR (125 MHz; DMSO-d_6): δ 166.60, 163.68, 157.75, 155.30, 140.58, 135.63, 132.10, 132.02, 128.09, 106.01, 105.56, 96.68, 19.64. HRMS (ESI-TOF) m/z: $[M + H]^+$ calculated for ($C_{13}H_{10}NO_3$) 260.0303, found 260.0301.

(Z)-1-((4-bromothiophen-2-yl)methylene)-6-methylfuro[3,4-c]pyridine-3,4(1H,5H)-dione (**12p**)

Following the general protocol 4-bromo-thiophene-2-carbaldehyde (380 mg, 1.98 mmoles) afforded **12p** in 395 mg (yield 65%). ^{1}H NMR (400 MHz; DMSO-d_6): δ 7.95 (s, 1H), 7.68 (s, 1H), 7.43 (s, 1H), 6.67 (s, 1H), 2.31 (s, 3H). ^{13}C NMR (125 MHz; DMSO-d_6): δ 163.79, 158.06, 156.27, 155.54, 142.34, 137.66, 133.12, 129.32, 110.43, 106.26, 104.66, 97.23, 20.10. HRMS (ESI-TOF) m/z: $[M + H]^+$ calculated for ($C_{13}H_9BrNO_3S$) 337.9481, found 337.9470.

(Z)-6-methyl-1-((4-phenylthiophen-2-yl)methylene)furo[3,4-c]pyridine-3,4(1H,5H)-dione (**12q**)

Following the general protocol 4-phenyl-thiophene-2-carbaldehyde **15a** (372 mg, 1.98 mmoles) afforded **12q** in 298 mg (yield 49%). ^{1}H NMR (500 MHz; DMSO-d_6): δ 12.20 (br. s, 1H), 8.17 (s, 1H) 7.83, (s, 1H), 7.73-7.72 (d, J = 6.85 Hz, 2H,), 7.46-7.43 (t, J_1 = 7.55 Hz, J_2 = 15.1 Hz, 1H,); 7.35-7.33 (d, J = 10.3 Hz, 2H), 6.72 (s, 1H), 5.13 (s, 1H), 2.34 (s, 3H). ^{13}C NMR (125 MHz; DMSO-d_6): δ 163.58, 157.70, 155.48, 155.19, 141.75, 141.08, 136.47, 134.28, 130.03, 129.05, 129.05, 127.61, 126.03, 126.03, 105.78, 105.62, 99.37, 96.72, 19.63. HRMS (ESI-TOF) m/z: $[M + H]^+$ calculated for ($C_{19}H_{14}NO_3S$) 336.0989, found 336.0710.

(Z)-6-methyl-1-((4-(pyridin-3-yl)thiophen-2-yl)methylene)furo[3,4-c]pyridine-3,4(1H,5H)-dione (**12r**)

Following the general protocol pyridine-3-yl-thiophene-2-carbaldehyde **15b** (374 mg, 1.98 mmoles) afforded **12r** in 207 mg (yield 34%). ^{1}H NMR (400 MHz; DMSO-d_6): δ 12.16 (br. s, 1H), 8.95 (s, 1H), 8.51-8.50 (d, J = 3.64 Hz, 1H,), 8.30 (s, 1H), 8.11-8.09 (d, J = 7.76 Hz, 1H), 7.87 (s, 1H), 7.46-7.43 (m, 1H), 7.31 (s, 1H), 6.72 (s, 1H), 2.31 (s, 3H). ^{13}C NMR (125 MHz; DMSO-d_6): δ 169.11, 163.53, 157.69, 155.60, 155.16, 148.54, 147.13, 141.32, 138.49, 133.37, 130.06, 129.77, 128.11, 123.97. 105.63, 105.52, 96.75, 19.65. HRMS (ESI-TOF) m/z: $[M + H]^+$ calculated for ($C_{18}H_{13}N_2O_3S$) 337.0641, found 337.0658.

(Z)-1-((4-(6-methoxypyridin-3-yl)thiophen-2-yl)methylene)-6-methylfuro[3,4-c]pyridine-3,4(1H,5H)-dione (**12s**)

Following the general protocol 6-methoxypyridine-3-yl-thiophene-2-carbaldehyde **15c** (433 mg, 1.98 mmoles) afforded **12s** in 336 mg (yield 51%). ^{1}H NMR (500 MHz; DMSO-d_6): δ 11.96 (bs, 1H); 8.43 (s, 1H); 8.15 (d, J = 4.2 Hz, 1H,), 7.91 (s, 1H), 7.31 (s, 1H,), 7.14 (s, 1H), 7.01 (d, J = 3.66 Hz, 1H), 6.72 (s, 1H), 3.89 (s, 3H) 2.29 (s, 3H). ^{13}C NMR (125 MHz; DMSO-d_6):

163.49, 159.56, 157.68, 155.59, 155.11, 153.98, 148.41, 142.66, 141.26, 140.02, 136.52, 130.03, 129.48, 110.67, 105.66, 103.67. 96.72, 79.03, 44.49, 28.08, 19.66. HRMS (ESI-TOF) m/z: $[M + Na]^+$ calculated for ($C_{19}H_{14}N_{20}O_2SNa$) 389.0566, found 389.2034.

(Z)-tert-butyl-4-(4-(5-((6-methyl-3,4-dioxo-4,5-dihydrofuro[3,4-c]pyridin-1(3H)-ylidene) methyl) thiophen-3-yl)pyridin-2-yl)piperazine-1-carboxylate (**12t**)

Following the general protocol tert-butyl 4-(5-(5-formylthiophen-3-yl)pyridin-2-yl)piperazine-1-carboxylate **15d** (738 mg, 1.98 mmoles) afforded **12t** in 390 mg (yield 43%). ^{1}H NMR (500 MHz; DMSO-d_6): δ 11.93 (bs, 1H); 8.42 (s, 1H); 8.15 (d, J = 4.8 Hz 1H,); 7.90 (s, 1H); 7.30 (s, 1H), 7.14 (s, 1H), 6.99 (d, J = 4.8 Hz, 1H,), 6.71 (s, 1H), 2.35 (s, 3H), 3.44 (m, 4H), 3.34 (m, 4H), 1.42 (s, 9H). ^{13}C NMR (125 MHz; DMSO-d_6):163.49, 159.56, 157.67, 155.59, 155.11, 153.97, 148.40, 142.65, 141.26, 140.02, 136.52, 130.02, 129.48, 110.67, 105.68, 105.53, 103.67, 96.72, 79.03, 44.48, 44.48, 28.08, 28.08, 28.08, 19.60. HRMS (ESI-TOF) m/z: $[M + H]^+$ calculated for ($C_{27}H_{29}N_4O_5S$) 521.1853, found 521.1876.

(Z)-3-((4-((E)-4-fluorostyryl)thiophen-2-yl)methylene)-4-methylfuro[3,4-c]pyridine-1,6(3H,5H)-dione (**12u**)

Following the general protocol (E)-4-(4-fluorostyryl)thiophene-2-carbaldehyde **15e** (460 mg, 1.98 mmoles) afforded **12u** in 245 mg (yield 36%). ^{1}H NMR (500 MHz; DMSO-d_6): δ 12.21 (br. s, 1H), 7.87 (s, 1H), 7.72 (s, 1H); 7.64-7.61 (t, J_1 = 7.55 Hz, J_2 = 13.75 Hz, 1H); 7.30 (s, 1H), 7.24-7.21 (dd, J_1 = 3.45 Hz, J_2 = 3.4 Hz, 3H), 7.14 (s, 1H,), 7.10 (s, 1H,), 6.74 (s, 1H), 2.34 (s, 3H). ^{13}C NMR (125 MHz; DMSO-d_6): δ 163.49, 159.56, 157.67, 155.59, 155.11, 153.97, 148.40, 142.65, 141.26, 140.02, 136.52, 130.02, 130.02, 129.48, 110.67, 110.67, 105.68, 103.67, 96.72, 79.03 19.66. HRMS (ESI-TOF) m/z: $[M + H]^+$ calculated for ($C_{21}H_{15}FNO_3S$) 380.0678, found 380.0779.

Synthesis of (Z)-6-methyl-1-((4-(piperidin-1-yl)thiophen-2-yl)methylene)furo[3,4-c]pyridine-3,4(1H,5H)-dione (**12v**)

Following the general protocol 4-(piperidin-1-yl)thiophene-2-carbaldehyde **15f** (386 mg, 1.98 mmoles) afforded **12v** in 437 mg (yield 71%). ^{1}H NMR (400 MHz; DMSO-d_6): δ 10.69 (s, 1H), 7.92-7.89 (m, 2H,), 7.26-7.25 (d, J = 4 Hz, 1H), 6.61 (s, 1H), 4.05 (s, 4H), 2.34 (s, 3H), 1.67 (s,

6H). ^{13}C NMR (125 MHz; DMSO-d_6): δ 167.31, 159.82, 158.82, 146.06, 143.57, 139.64, 132.09, 131.38, 130.38, 128.18, 95.65, 48.50, 48.50, 25.36, 25.36, 23.51, 18.99. HRMS (ESI-TOF) m/z: $[M + H]^+$ calculated for ($C_{18}H_{19}N_2O_3S$) 343.1811, found 343.1851.

General procedure for the syntheses of 15a-e.

To a stirred solution of 4-bromothiophene-2-carbaldehydes (1eq), in 1, 4 dioxane (10 vol), added corresponding arylboronicacids (1.2 eq), followed by aqueous (2M) K_2CO_3 (3 eq), purged with argon gas for 15 min, then Bis(triphenylphosphine)palladium(II) dichloride (0.05 eq) was added and the reaction mixture was heated at 100° C for 14 h. Once TLC indicates complete consumption of the starting material, the reaction mixture was allowed to cool to room temperature then filtered through celite, quenched with 20 volume of brine solution, extracted with ethyl acetate (2 × 10 vol), evaporated to dryness to give the crude substituted thiophene aldehydes (**15a-e**), which were used in the above reaction as such.

General procedure for the synthesis of 15f.

To a stirred solution of 4-bromothiophene-2-carbaldehyde (200 mg, 1 mmol), in dimethyl formamide (10 mL), was added piperidine (90 mg, 1.1 mmol) and solid potassium carbonate (150 mg, 1.1 mmol). The reaction mixture was heated at 110°C for 6h. Once TLC indicates complete consumption of the starting material, the reaction mixture was allowed to cool to room temperature then filtered through celite, quenched with 20 mL of water, extracted with ethyl acetate (2 × 10 mL), which was then evaporated to dryness to give the crude **15f**, which was used in the above reaction as such.

Pharmacological protocols

***In vitro* inhibition screening assay of α-glucosidase (yeast origin)**

The effectiveness of the compounds on inhibition of α-glucosidase (yeast origin) was assessed in 96-well plates using the respective substrates and buffering systems according to the procedure reported by Ferreres *et al*.[23] Prior to assays, all the test compounds were dissolved in a suitable solvent, dimethylsulfoxide (DMSO) and eventually diluted to attain the desired concentration. The absorbance was measured spectrophotometrically at 400 nm (Epoch reader; version

2.00.18). The decrease in absorbance (ΔA) was compared with that of control (buffer instead of test compound) to compute the inhibitory profile of enzyme. The data used for the determination of IC_{50} concentrations were fitted by non-linear regression fitting and the variance analysis was carried out by using MINITAB 15 software (trail version). The concentration of inhibition required for 50% of α-glucosidase activity under the assay conditions was defined as the IC_{50} value. The half maximal inhibitory (IC_{50}) concentrations were determined from two independent assays, performed in duplicate. Acarbose, an eminent α-glucosidase inhibitor, was employed as a positive control.

$$\text{Inhibition (\%)} = \Delta Acontrol - \Delta Asample) / \Delta Acontrol \times 100\%$$

One unit (IU) is defined as the amount of enzyme (α-glucosidase) which produces 1 μmol of PNP (*p*-nitro phenol) per min at 37°C under the respective reaction conditions described below.

In brief, the assay condition is as follows:

α-glucosidase inhibition (AGI)

For AGI, 100μL of *p*-nitrophenol-α-D-glucopyranoside substrate (2mM, PNP-Glu is dissolved in 2mM phosphate buffer at a pH of 7.2) and different concentrations of the test compounds were taken in 96-well plates. Then the final volume of the reaction mixture was made up to 200μl with 2mM phosphate buffer (pH 7.2). The hydrolytic reaction was commenced by the addition of α-glucosidase enzyme (0.5 IU/mL) (obtained from Sigma Aldrich, Bangalore) and the plates were incubated at 37°C for 15 min. The reaction was terminated by the addition of 50μL of 2N Na_2CO_3 solution.

Inhibition-kinetics

The kinetic mode of inhibition of the highest active compounds against α-glucosidase (yeast origin) was determined by preparing a series of test solutions in which the concentration of the respective substrate was varied in the presence of different concentrations of the inhibitors. The mode of inhibition (i.e. competitive, non-competitive, uncompetitive or mixed-type) of the screened compounds was determined on the basis of the inhibitory effects on K_m (Michaelis constant: It is defined as the substrate concentration at half of the maximum velocity of the

enzyme) and V_{max} (maximum reaction velocity) of the enzyme.[22] These studies were computed using the primary (Lineweaver-Burk plot) plots, which are the double reciprocal plots of enzyme reaction velocities (1/V) versus substrate concentrations (1/[S]). Analysis of the same data by secondary plots of slope versus [Inhibitor] and Y-intercept versus [Inhibitor] were also performed. The Lineweaver-Burk (LB) equation follows as,

$$\frac{1}{v} = \frac{1}{V_{max}} + \frac{K_m}{V_{max}} \times \frac{1}{[S]}$$

Molecular docking Methodology

Homology modelling

The sequence of alpha-glucosidase was downloaded from Uniprot (ID: P10253). Blastp against protein data bank database was perform in order to identify the template for sequence alignment. Human Maltase-Glucoamylase (PDB ID: 2QLY, 3L4T) were showing good similarity to our query sequence. Residues starting from 89 are aligning to these PDB and showing 44% identity. So we select these two protein structure to model alpha-glucosidase using homology modelling. The homology model of alpha-glucosidase was built using Modeller v9.14. Three models were generated using Modeller v9.14 and model having best DOPE score is selected for further refinement. Modelled structure consist of certain loops structure that are further refined using ModLoop server. The energy of the refined model was minimized using maestrov10 using Force Field OPLS2005. The steriochemical quality of this model is validated by Ramachanadran plot. More than 99.3 % residues are in favored and allowed regions and only 0.7% (6 residues) are in outlier region (Figure 1).

Preparation of modelled alpha glucosidase protein structure

Protein preparation was performed using protein preparation wizard of maestro v10 in which assign bond orders, addition of hydrogens, create di-sulfide bonds were done. After that H-bond assignment were optimize using PROPKA at pH 7.0. Finally the energy of the protein was minimized using OPLS2005 force field.

Ligand preparation

The 2D structure of **12p** and natural substrate of alpha glucosidase i.e. Acarbose were built using MOE-Builder tool. After this various 3D conformation was search using conformational search tool in MOE. The conformations having least energy were selected for docking studies.

X-ray crystal structure determination

X-ray diffraction data for **12p** was collected at room temperature using *Mo* K_α (λ = 0.71073 Å) radiation on a Bruker D8 Venture diffractometer system equipped with dual micro focus sources and Photon 100 CMOS detector. The data collection strategy employed for **12p** was omega and phi scan. The crystal structure was solved by direct method using the SHELXS program implemented in SHELXTL package and refined by full-matrix least squares methods using SHELXL-2014.[24] The non-hydrogen atoms were located in successive difference Fourier syntheses and refined with anisotropic thermal parameters. All the hydrogen atoms were placed at the calculated positions and refined using a riding model with appropriate HFIX commands. The structural details can be found from the deposited CIF with CCDC number 1401263.

Acknowledgements

The authors would like to sincerely appreciate Shiv Nadar University for funding.

Supplementary materials

The deposited CIF with CCDC 1401263 (**12p**) contains the supplementary crystallographic data for this paper. This data can be obtained free of charge from The Cambridge Crystallographic Data Centre via http://www.ccdc.cam.ac.uk/data_request/cif. Supplementary data including NMR spectra and LCMS related to this article can be found with the online version of the paper.

References

1. Y. Shi, F. B. Hu, *The Lancet*, **2014**, *383*, 1947–8.
2. S. Wild, G. Roglic, A. Green, R. Sicree, H. King, *Diabetes Care* **2004**, *27*, 1047-1053.
3. D. V. Nguyen, L. C. Shawand, M. B. Grant, *Front. Endocrinol. (Lausanne)* **2012**, 3, 1-7.
4. S. E. Nissen, K. Wolski, *N. Engl. J. Med*. **2007**, *356*, 2457–71.

5. (a) J. B. Buse, D. C. Klonoff, L. L. Nielsen et al. *Clin. Ther.* **2007**, *29*, 139–53. (b) F. X, Pi-Sunyer, A. Schweizer, D. Mills, et al. *Diabetes Research Clinical Practice* **2007**, *76*, 132–8.
6. D. Cota, G. Marsicano, M. Tschop, et al. *J Clin. Invest*. **2003**, *112*, 423–31.
7. K. C. Maki, M. L. Carson, M. P. Miller, M. Turowski, M. Bell, D. M. Wilder, M. S. Reeves, *Diabetes Care*, **2007**, *30*, 1039-1043.
8. H. A. Ernst, et al., *J. Mol. Biol.* **2006**, *358*, 1106-1124.
9. (a) B. Henrissat, *Biochem. J*. **1991**, 280, 309-316. (b) B. Henrissat, A. Bairoch, *Biochem. J.* **1993**, *293*, 781-788.
10. (a) A. J. Krentz, C. J. Bailey, *Drugs*, **2005**, *65*, 385-411. (b) D. O. Schmidt, W. Frommer, L. Muller, E. Truscheit, *Natunlinenschafien* **1979**, *66*, 584-585. (c) W. Puts, U. Keup, I.J.P. Krause, G. Thomas, F. HoO'meister, *Naturwissenschafien* **1977**, *64*, 536-537.
11. N. Asano, *Curr. Top. Med. Chem*. **2003**, *3*, 471-484.
12. T. Tanaka, R. Uehara, K. Nishida, I. Kouno, *Phytochemistry* **2005**, *66*, 675-681.
13. T. K. Tabopda, J. Ngoupayo, P. K. Awoussong, A. Mitaine-Offer, M. S. Ali, B. T. Ngadjui, M. Lacaille-Dubois, *J. Nat. Prod*. **2008**, *71*, 2068-2072.
14. H. Oe, S. Ozaki, *Biosci. Biotechnol. Biochem*. **2008**, *72*, 1962-1964.
15. M. Shibano, D. Tsukamoto, A. Masuda, Y. Tanaka, G. Kusano, *Chem. Pharm. Bull*. **2001**, *49*, 1362-1365.
16. D. Zhang, M. Fu, S. Gao, J. Li, *Evidence-based Complementary and Alternative Medicine*, **2013**, p. 16. Article ID 636053, http://dx.doi.org/10.1155/2013/636053
17. N. J. Pawar, V. S. Parihar, S. T. Chavan, R. Joshi, P. V. Joshi, S. G. Sabharwal, V. G. Puranik, D. D. Dhavale, *J. Org. Chem*. **2012**, 77, 7873-7882.
18. M. Khan, M. Yousaf, A. Wadood, et al., *Bioorg. Med. Chem*. **2014**, *22*, 3441-3448.
19. (a) T. Narender et al. *Eur. J. Med. Chem*., **2013**, *63*, 162-169. (b) W. Hou, Y. Li, Q. Zhang, X. Wei, A. Peng, L. Chen, Y. Wei, *Phytother. Res*. **2009**, *23*, 614-618.
20. (a) M. Fioravanti, L. Flicker, *Cochrane Database Syst. Rev.* 2001, 4, CD003159. (b) M. Fink, P. Irwin, *Clinical Pharmacology and Therapeutics* **1981**, *30*, 336–42. (c) F.

Passamonti, M. Lazzarino, *Leukemia & Lymphoma* **2003**, *44*, 1483–1488. (d) P. N. Mohite, A. M. Bhatnagar, *The Internet Journal of Surgery* ***2009***, *21*. ISSN 1528-8242.

21. H. Lineweaver, D. Burk, *J. Am. Chem. Soc.* **1934**, *56*, 658–666.
22. B. T. Burlingham, T. S. Widlanski, *J. Chem. Edu*. **2003**, *80*, 214-218.
23. F. Ferreres, A. Gil-Izquierdo, J. Vinholes, S. T. Silva, P. Valentao and P. B. Andrade, *Food Chem*, **2012**, *134*, 894-896.
24. Sheldrick, G. M. SHELXTL Version 2014/7. http://shelx.uni-ac.gwdg.de/SHELX/index.php.